



САМАРСКИЙ УНИВЕРСИТЕТ
SAMARA UNIVERSITY

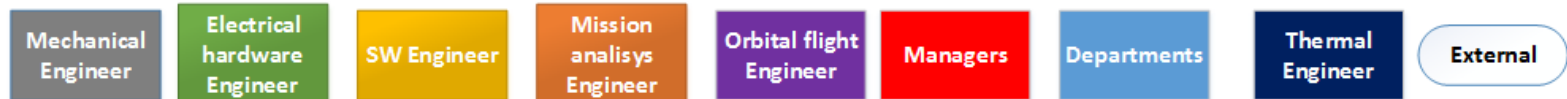
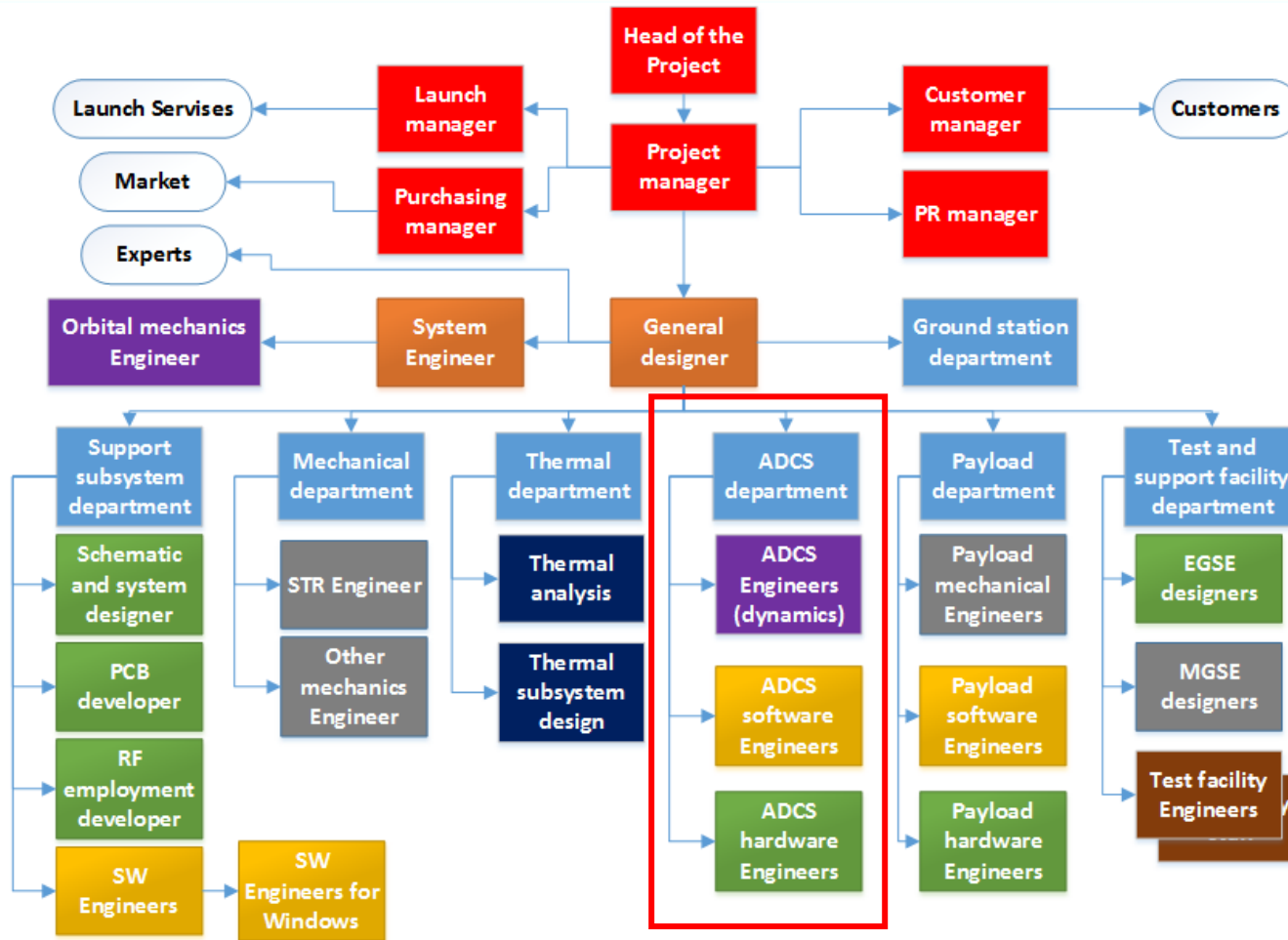
Methods and Algorithms for Nanosatellite Attitude Control

Dr. Petr Nikolaev

Samara, 2023

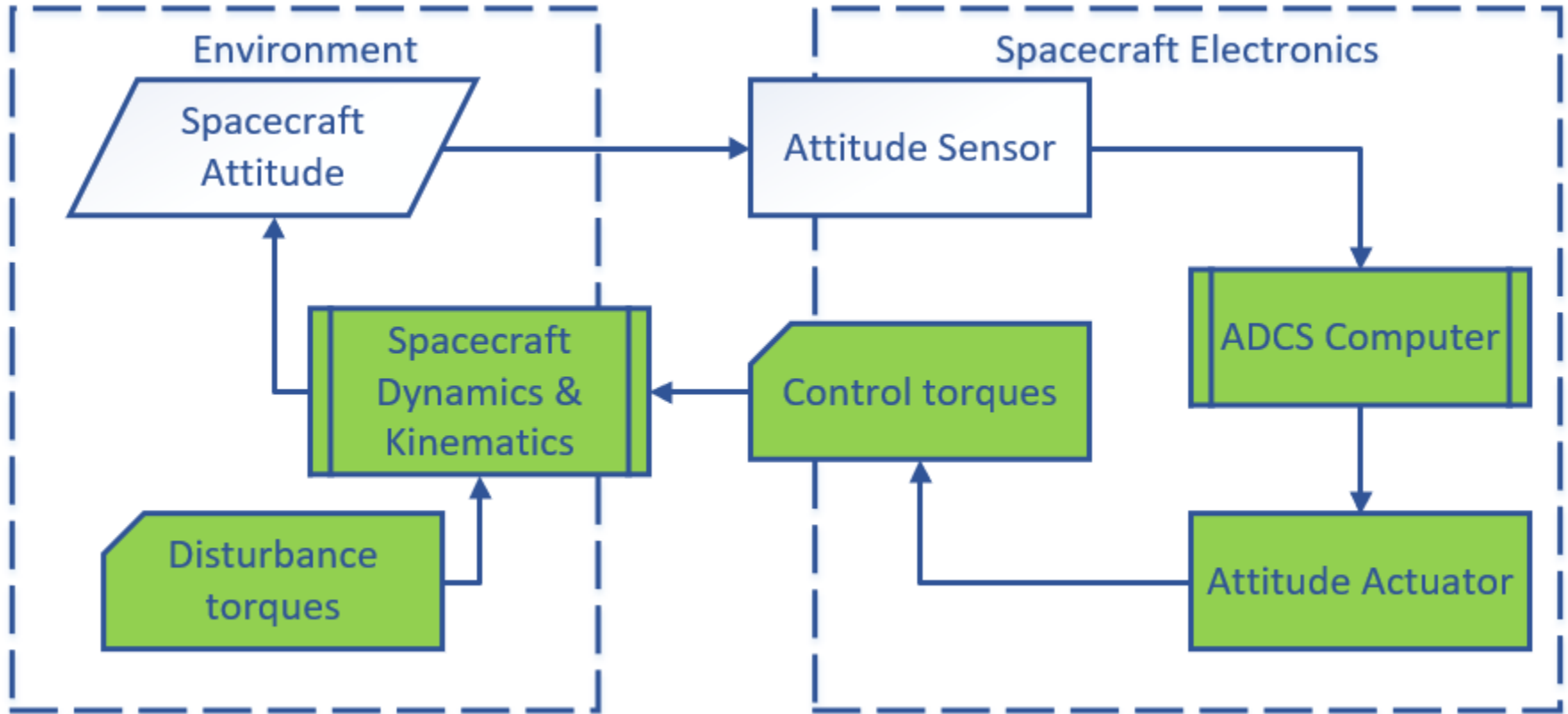


Nanosatellite Development





ADCS Structure



ADCS closed-loop control system



Vector equation

$$\frac{d\bar{h}_0}{dt} + \bar{\omega} \times \bar{h}_0 = \bar{M}_0^e,$$

where $\bar{h}_0 = I\bar{\omega}$ - angular momentum vector;
 \bar{M}_0^e - the main moment of external forces relative to the center of mass;
 $\bar{\omega}$ - absolute angular velocity;
 I - inertia tensor.

In the projections to the main central axes of inertia of the CS Ox, Oy, Oz, (attitude dynamics equations)

$$I_x \dot{\omega}_x + (I_z - I_y) \omega_y \omega_z = M_{xg} + M_{xa} + M_{xctrl}$$

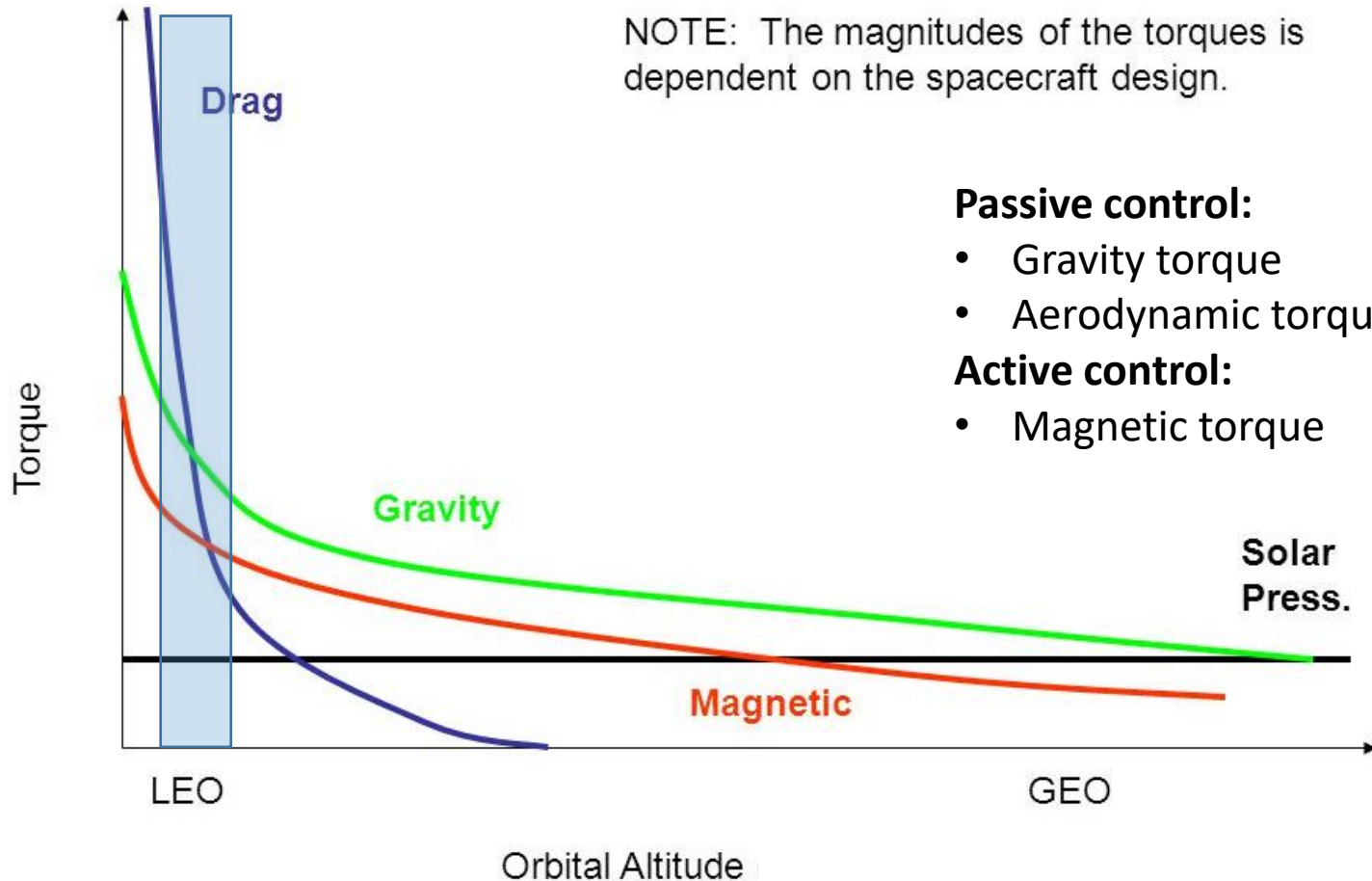
$$I_y \dot{\omega}_y + (I_x - I_z) \omega_z \omega_x = M_{yg} + M_{ya} + M_{yctrl}$$

$$I_z \dot{\omega}_z + (I_y - I_x) \omega_x \omega_y = M_{zg} + M_{za} + M_{zctrl}$$

where $\omega_x, \omega_y, \omega_z$ - projections of angular velocity vector on the axis Ox, Oy, Oz;
 I_x, I_y, I_z - main central moments of inertia;
 M_x, M_y, M_z - projections of main moment of external forces on the axis Ox, Oy, Oz.



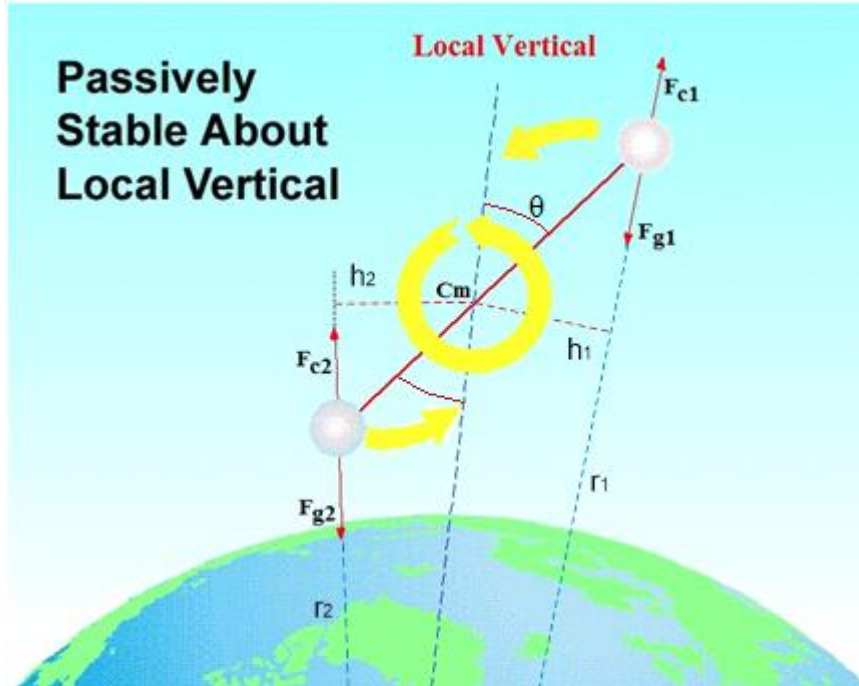
Moments of External Forces



Typical torques on a small spacecraft as a function of orbital altitude above Earth's surface



Gravity Gradient



$$m_1 = m_2,$$

$$r_2 < r_1, \quad F_{g2} > F_{g1},$$

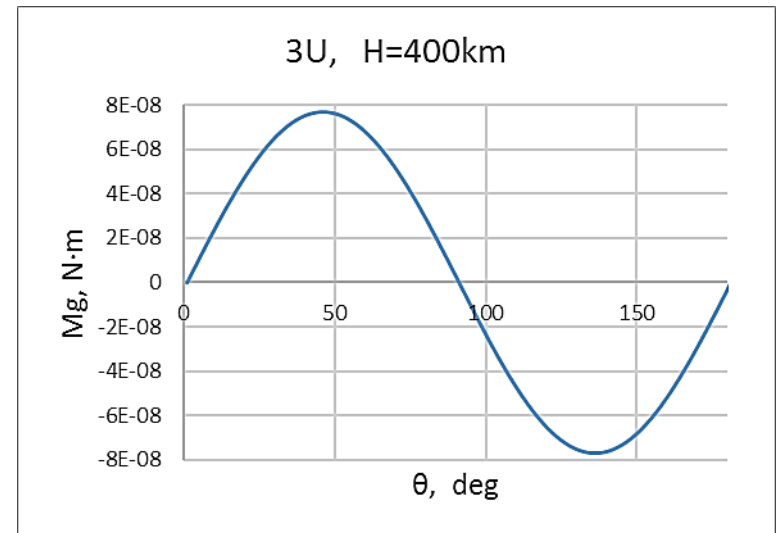
$$h_2 > h_1,$$

$$M_2 = F_{g2}h_2 > M_1 = F_{g1}h_1$$

$$M_{x_g} = \frac{3\mu}{R^3} (I_z - I_y) a_{22} a_{32}$$

$$M_{y_g} = \frac{3\mu}{R^3} (I_x - I_z) a_{32} a_{12}$$

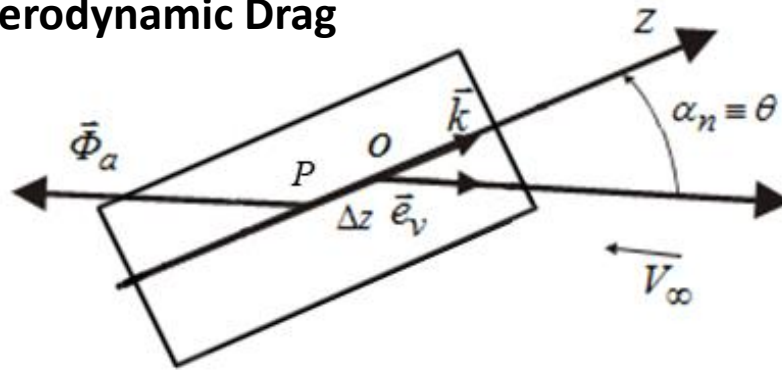
$$M_{z_g} = \frac{3\mu}{R^3} (I_y - I_x) a_{12} a_{22}$$



Gravitational moment M_g
for CubeSat 3U



Aerodynamic Drag



$$\vec{M}_{OA} = \vec{r}_D \times \vec{\Phi}_a = \frac{1}{2} \rho V^2 C(\alpha_n) \vec{e}_v \times \vec{k},$$

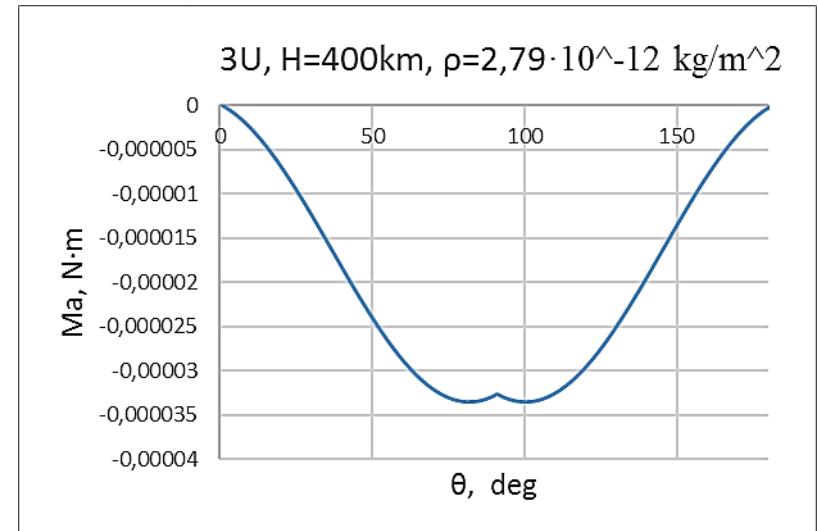
where ρ is the atmospheric density, V is the upstream velocity, $C(\alpha_n)$ is drag coefficient, φ is the angle of proper rotation, α is the attack angle, $S(\alpha_n)$ is projection of the cross-sectional area onto a plane perpendicular to the upstream velocity vector, $\Delta z(\alpha_n)$ is projection of the static stability margin on the upstream velocity vector.

$$M_{x_a} = \frac{1}{2} \rho V^2 C(\alpha_n) \cos \varphi \sin \alpha_n,$$

$$M_{y_a} = \frac{1}{2} \rho V^2 C(\alpha_n) \sin \varphi \sin \alpha_n,$$

$$M_{z_a} = 0.$$

$$C(\alpha_n) = C_{x\alpha} S(\alpha_n) \Delta z(\alpha_n)$$



Aerodynamic moment M_a
for CubeSat 3U



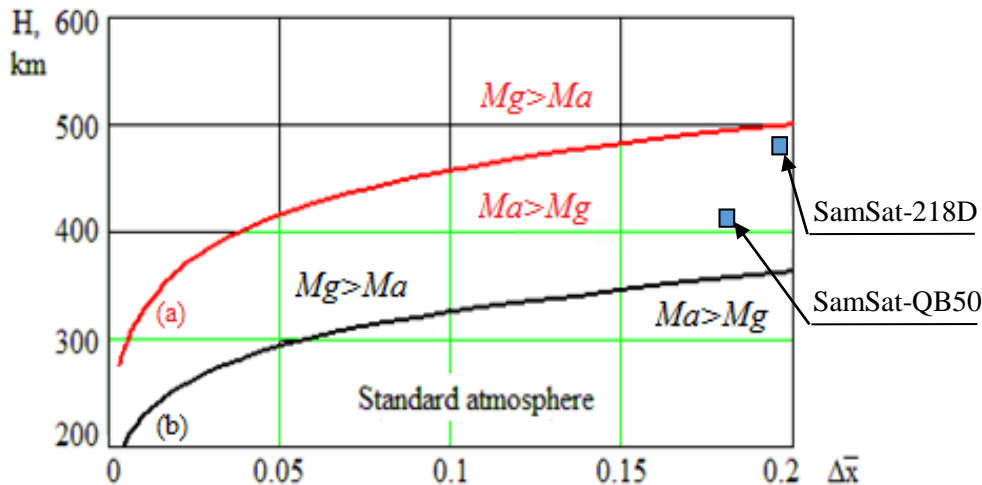
Features of Nanosatellites' Motion in Low Orbits

1. The **ballistic coefficient** of the spacecraft is inversely proportional to the its linear dimension, thus the **value of the ballistic coefficient of nanosatellite is greater than for a satellite with large dimensions and mass** (with the same density), and, therefore, the **lifetime in the orbit of nanosatellite is shorter**.

$$\frac{\sigma_c}{\sigma_m} = N \frac{\gamma_m}{\gamma_c}$$

where γ_c is the density of the nanosatellite, γ_m is the density of the minisatellite, N is a ratio of the edges of the minisatellite and the nanosatellite

2. Since the **magnitude of the angular acceleration** due to the aerodynamic moment of the satellite is inversely proportional to the square of the its linear dimension, then the angular acceleration due to the aerodynamic moment acting on nanosatellite is much higher than the satellite with large dimensions and mass (at the same values of the relative margin of static stability and density).



- The area of altitudes H and the relative margin of static stability, where the aerodynamic moment Ma exceeds the gravitational moment Mg for:
- (a) - the nanosatellite CubeSat 3U;
 - (b) - the satellite whose dimensions are 10 times larger than the dimensions of the nanosatellite CubeSat 3U.
- SamSat-218D: $H_0 = 486$ km, $\mathbf{Ma / Mg = 2.3}$;
 SamSat-QB50: $H_0 = 405$ km, $\mathbf{Ma / Mg = 10}$



The Relationship Between Ballistic Coefficient and CubeSat Attitude

The **ballistic coefficient** of nanosatellite SamSat-218D (CubeSat3U):

$$\sigma(\alpha, \varphi) = c_0 (|\cos \alpha| + k_s \sin \alpha (|\sin \varphi| + |\cos \varphi|)) S / m ,$$

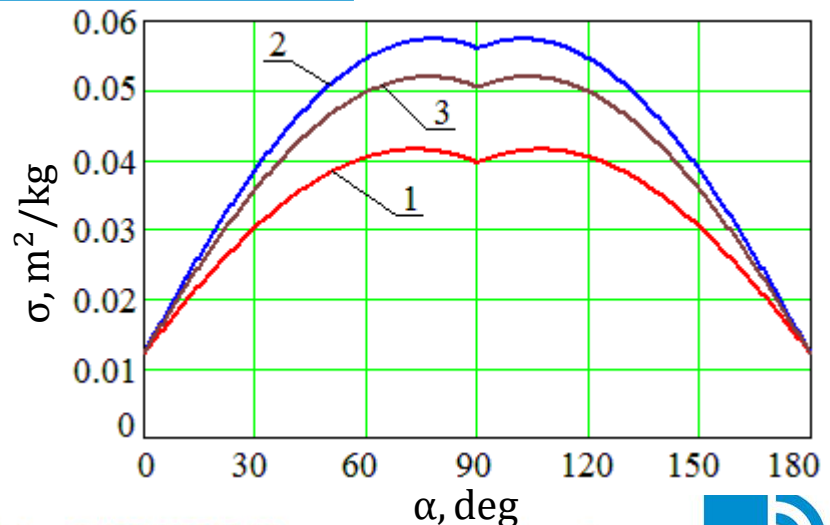
where $\alpha = \alpha_s$ is the angle of attack; φ is the proper rotation angle;
 m is the satellite mass; $c_0 = 2.2$ is the drag force coefficient;
 S is the characteristic area;
 k_s is the ratio of the one side surface area to the characteristic area.

The **ballistic coefficient** averaged over the angle of proper rotation

$$\sigma(\alpha) = c_0 (|\cos \alpha| + \frac{4k_s}{\pi} \sin \alpha) S / m .$$

Dependence of SamSat-218D ballistic coefficient on angle of attack α and angle of proper rotation φ :
1 - $\varphi = 0^\circ$; 2 - $\varphi = 45^\circ$;
3 - averaged over the angle of proper rotation.

$$\frac{\sigma_{\max}(\alpha, \varphi)}{\sigma_{\min}(\alpha, \varphi)} = 4.75$$





Possible Attitude Motion Modes (Uncontrollable Planar Motion)

Energy integral of system in planar motion ($h=\text{const}$ case)

$$\frac{\dot{\alpha}^2}{2} + a \cos \alpha + c \cos^2 \alpha = \text{const} = E_0$$

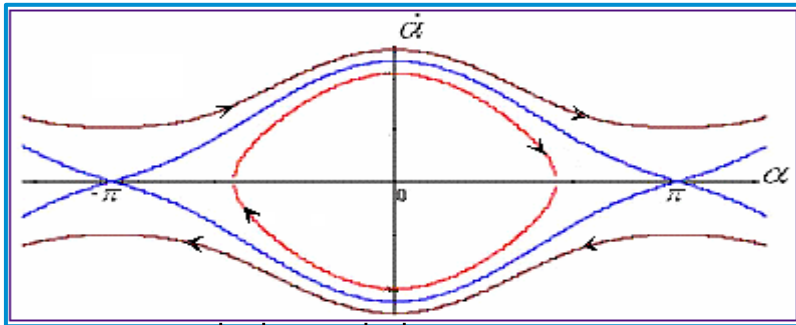
Where α is the angle of attack; h is the flight altitude;

$n = \sqrt{k/R^3}$ is the NS orbital velocity;

$c(h) = \frac{3(I - I_x)n^2}{2I}$ is the coefficient reflecting the gravitational moment;

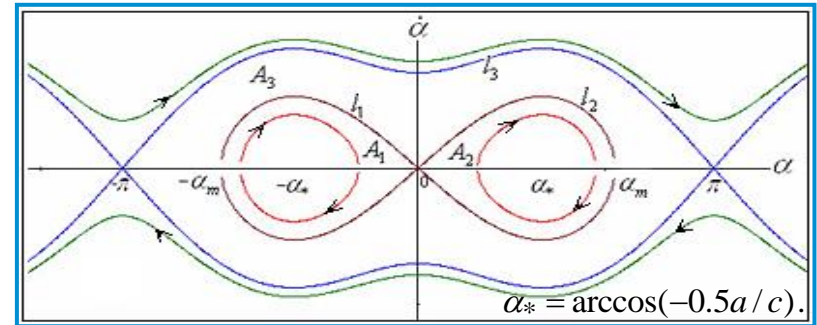
$a(h) = m_a(\alpha) \frac{2I S l q}{I}$; is the coefficient reflecting of restoring aerodynamic moment

Phase portraits



$$|a| \geq 2|c|, a < 0.$$

Rotational motion mode : $E_0 > -a + c$.



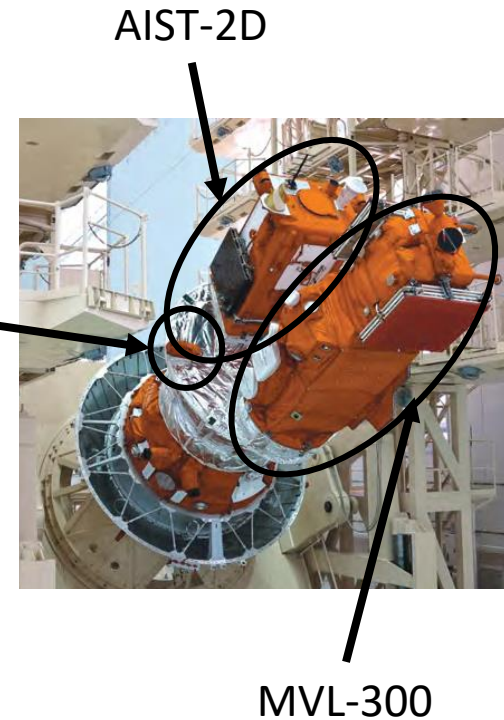
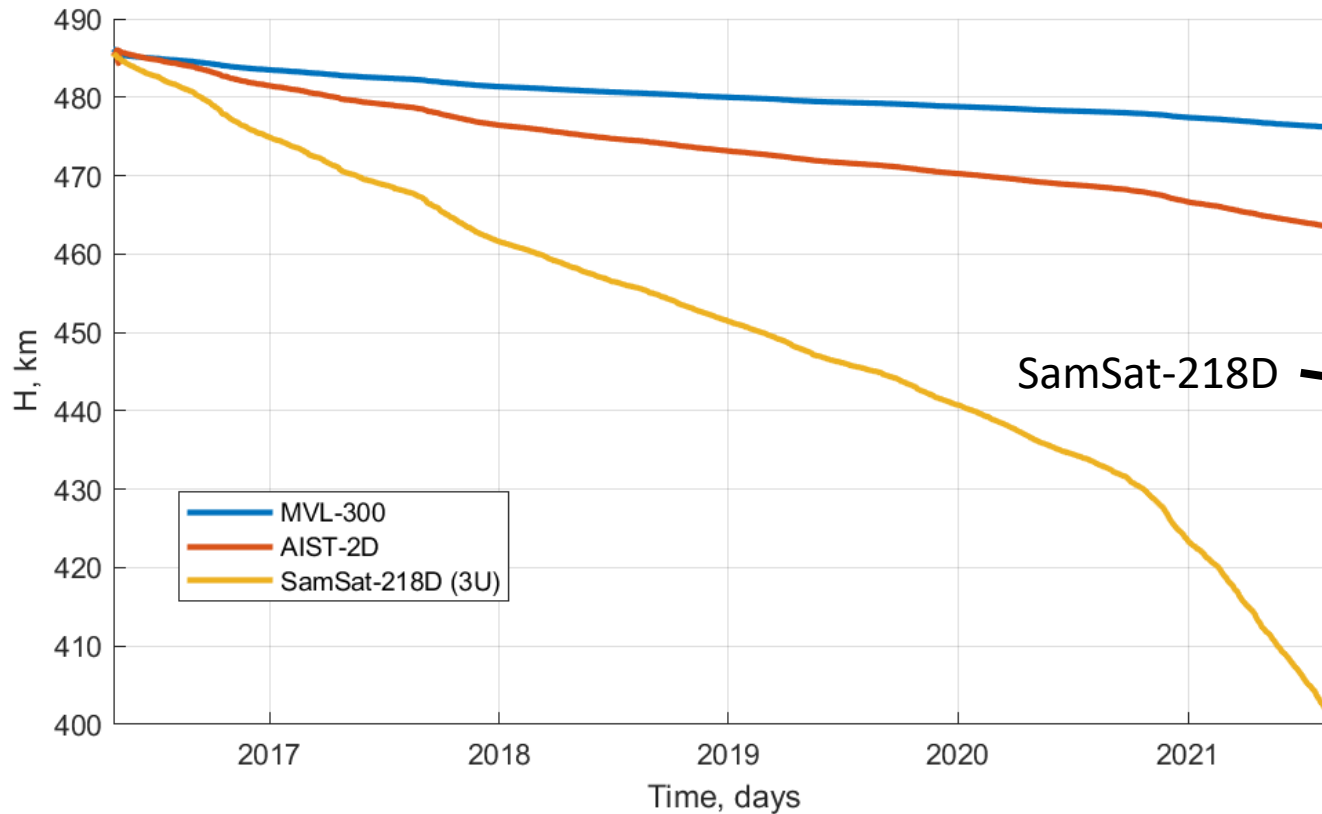
$$c > 0.5|a|, c > 0, a < 0.$$

Rotational motion mode : $E_0 > -a + c$.
Oscillates motion mode with respect to the equilibrium position $\alpha=0$: $-a + c > E_0 > a + c$.





Changes in Satellites Altitude by NORAD TLE Files



The changes in altitude of the orbit of satellites MVL-300, Aist-2D and SamSat-218D, which were launched almost simultaneously on April 28, 2016 from Vostochny Cosmodrome into near-circular orbit with an average altitude of $H = 486$ km. Time duration 28 months.

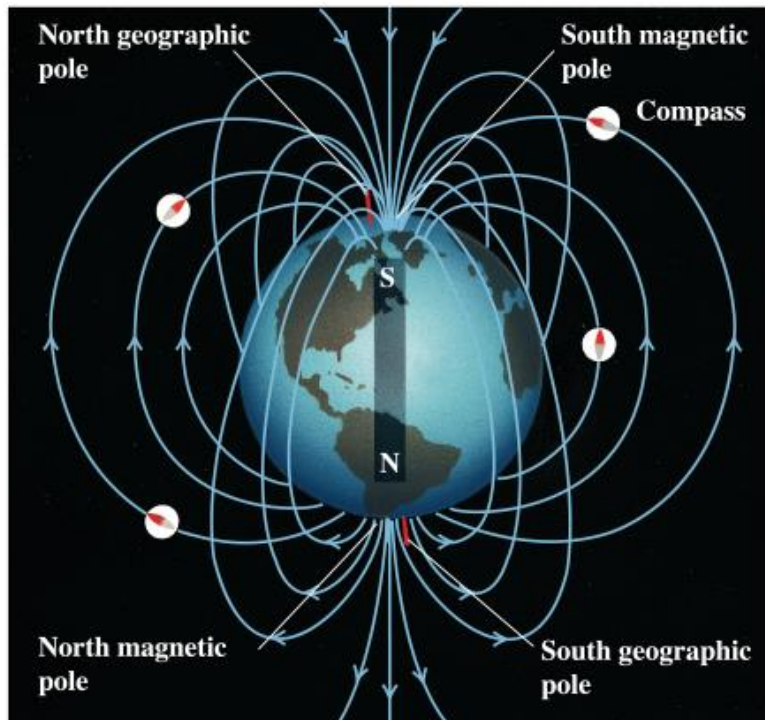
The decrease in the altitude of the SamSat-218D nanosatellite is **2.5 times** larger than that of the Aist-2D satellite and it is **5.8 times** larger than that of the MVL-300 satellite.



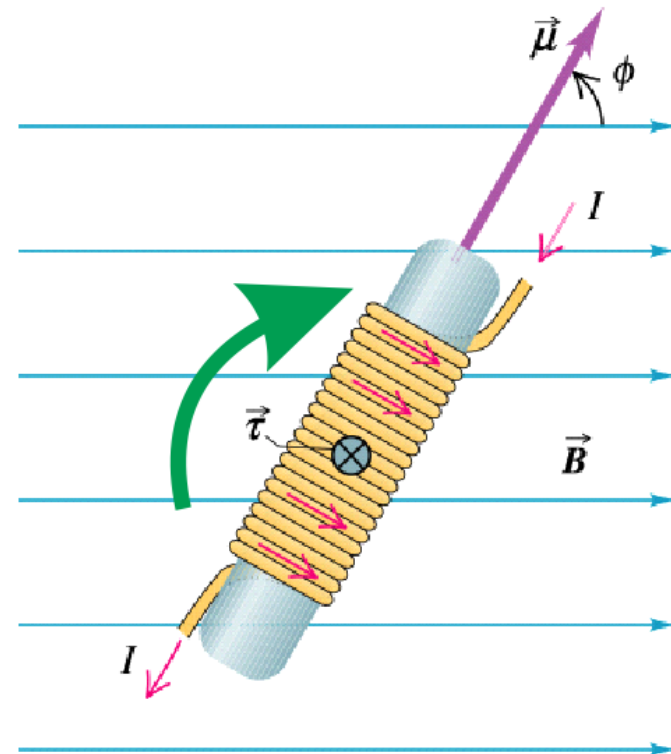
Magnetic moment

$$\tau = \mu \times B$$

From the right-hand rule we see that the torque vector τ is directed into the page or screen. The torque tends to rotate the solenoid in a clockwise direction.



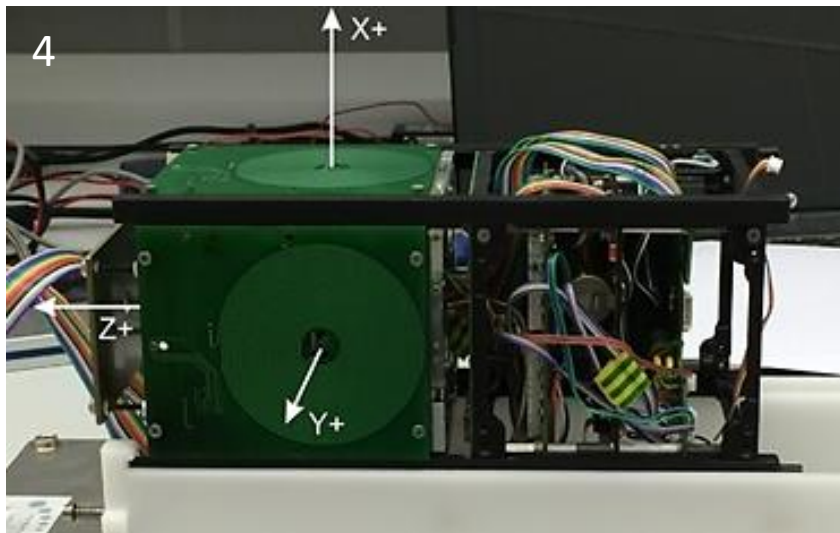
Copyright © Addison Wesley Longman, Inc.



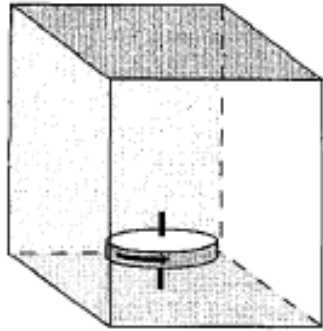
Copyright © Addison Wesley Longman, Inc.



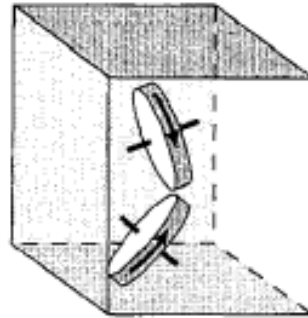
Hardware of ADCS. Attitude Actuators



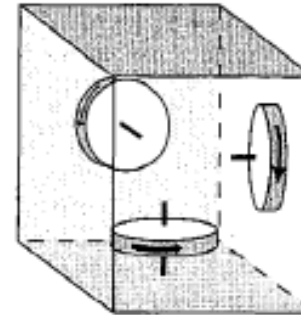
- 1, 2. ISIS Magnetorquer board
(nominal 0.2Am^2 actuation per actuator)
3, 4. SamSat flat magnetorquer coil
(nominal 0.05Am^2 actuation per actuator)



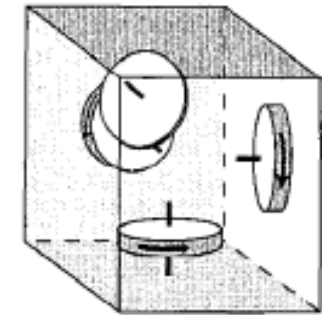
(A) One-Wheel System



(B) Two-Wheel System



(C) Three-Wheel System

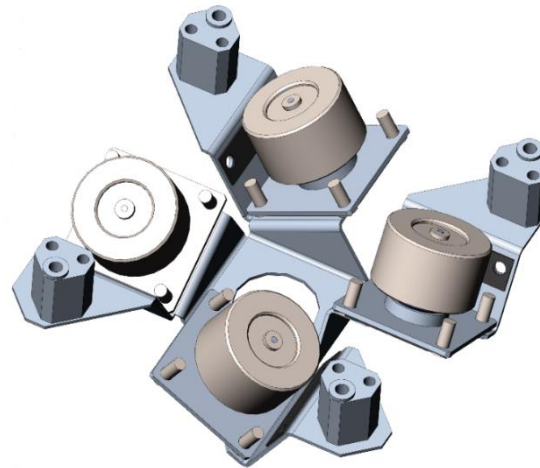


(D) Four-Wheel System

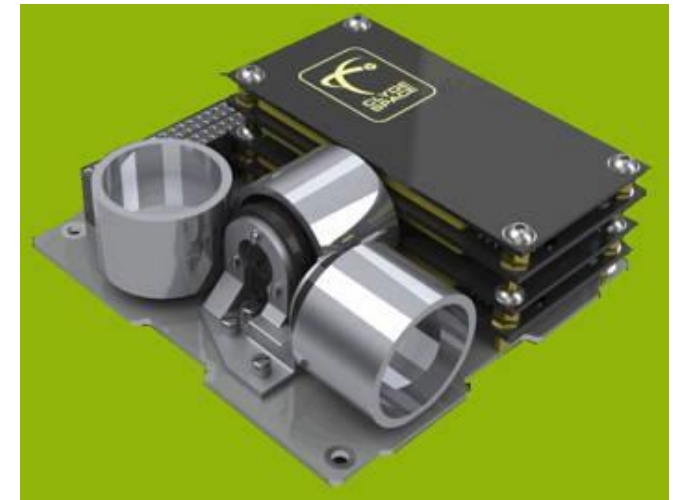
Options for reaction wheels configuration (Wertz, 2001)



One reaction wheel
© Clyde Space



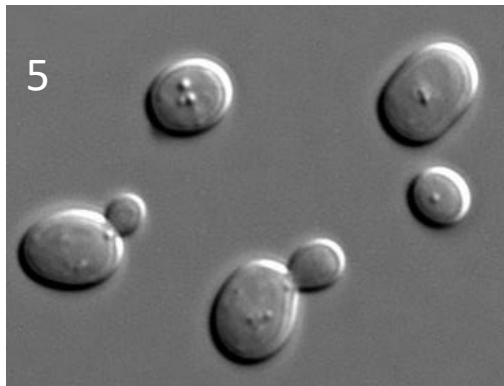
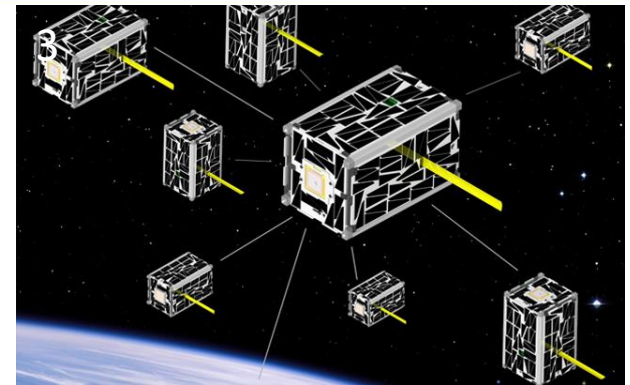
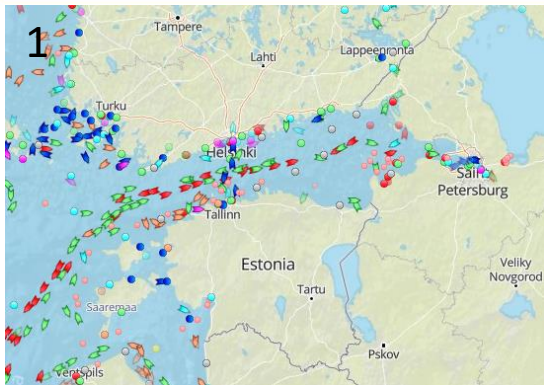
Four-Wheel System



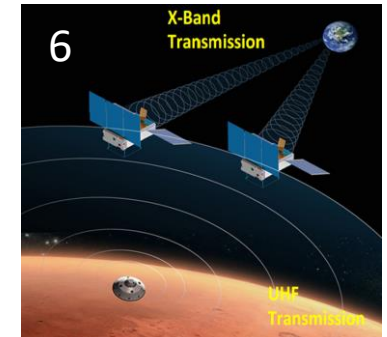
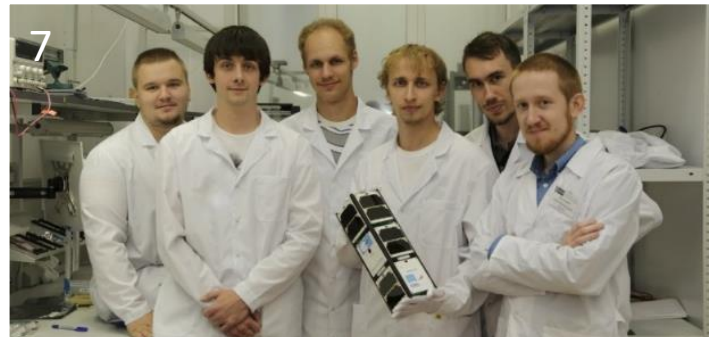
Three-axis attitude control system
© Clyde Space



Nanosatellites Missions



1. Automatic identification system
2. Remote sensing
3. Formation flying
4. Experimental development of new technologies
5. Science
6. Communication
7. Education





Nanosatellite Deployment Conditions



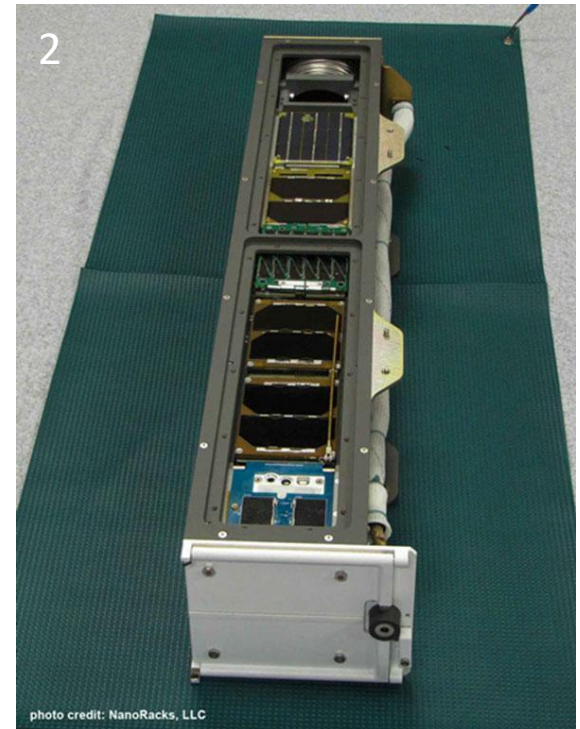
SRC Progress deployer

Initial angular velocity*: $\omega_{3\sigma} = 10^\circ/s$

QB50 project requirements

Nominal conditions: $\omega_{3\sigma} = 50^\circ/s$

Off-nominal conditions: $\omega_{3\sigma} = 90^\circ/s$



1. SRC
Progress
deployer

2. NanoRacks
deployer

* **Yudincev V.V.** Dinamika otdeleniya nanosputnika formata cubesat ot transportno-puskovogo kontejnera // Polet. Obshcherossiyskij nauchno-tekhnicheskij zhurnal. -2015, vol. 8-9, pp. 10-15

Moskovskoye shosse, 34, Samara, 443086, Russia, tel.: +7 (846) 335-18-26, fax: +7 (846) 335-18-36, www.ssau.ru, e-mail: ssau@ssau.ru

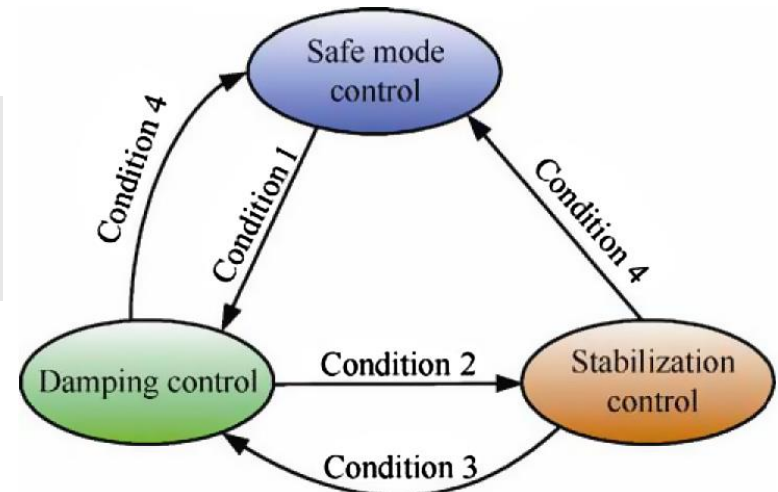




Switch conditions for each control mode

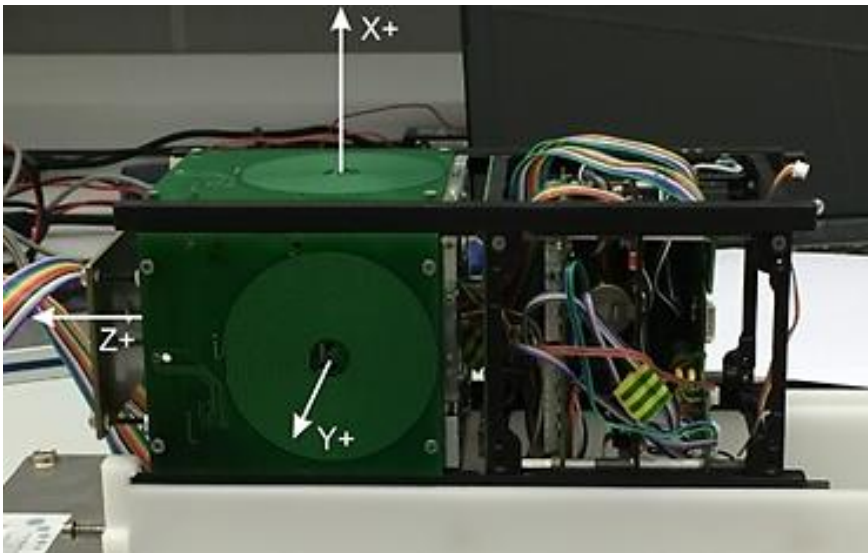
Tian Tuo 1

Condition	Switch condition
Condition 1	Launch separation successfully Electric energy sufficient
Condition 2	In sunlight area Attitude angular velocity error: roll/yaw $<0.15^\circ/\text{s}$, pitch $<0.35^\circ/\text{s}$ Attitude angular error: roll/yaw $<80^\circ$, pitch $<20^\circ$ Conditions 1, 2 and 3 last for more than 10 s
Condition 3	Attitude angular velocity error over $0.8^\circ/\text{s}$ Condition 1 lasts for more than 10 s
Condition 4	Attitude determination algorithm divergence Electric energy insufficient Ground telemetry command



Attitude control flow chart of nanosatellite - "Tian Tuo 1"

*<https://www.sciencedirect.com/science/article/pii/S1000936113002112?via%3Dihub>



B-dot method

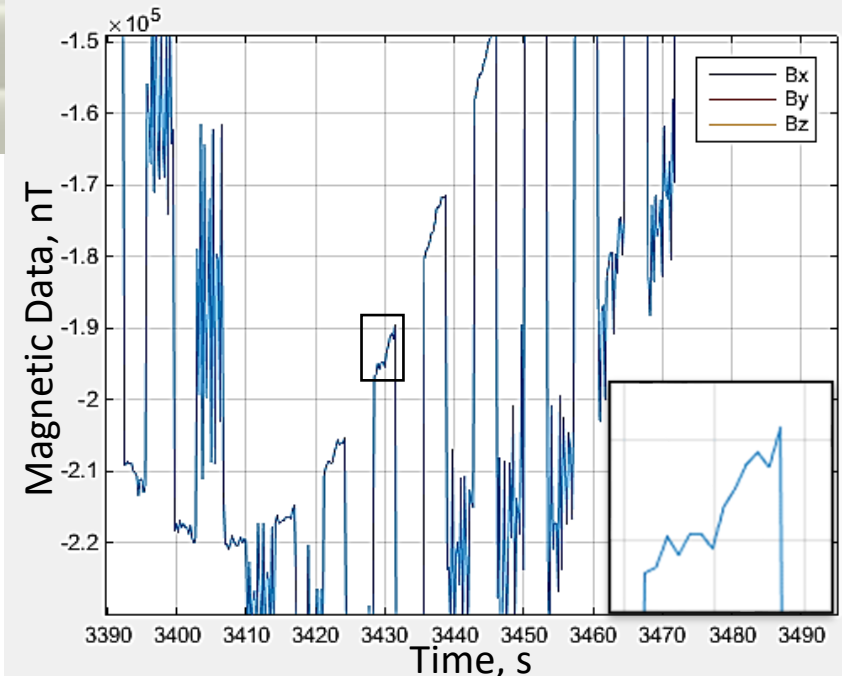
$$\bar{m} = -k\dot{\vec{B}}$$

$$\bar{m} = -JS\bar{n}$$

$$J\bar{n} = -\frac{k}{S}\dot{\vec{B}}$$

B-dot method has a low amount of calculation required and fast convergence speed, which applies to the despun stage after deployment.

B-dot method is severely affected by the magnetometer measurement noise.





Ex 1. Division into repetitive steps

Computing of \dot{B} phase:

Second-degree polynomial

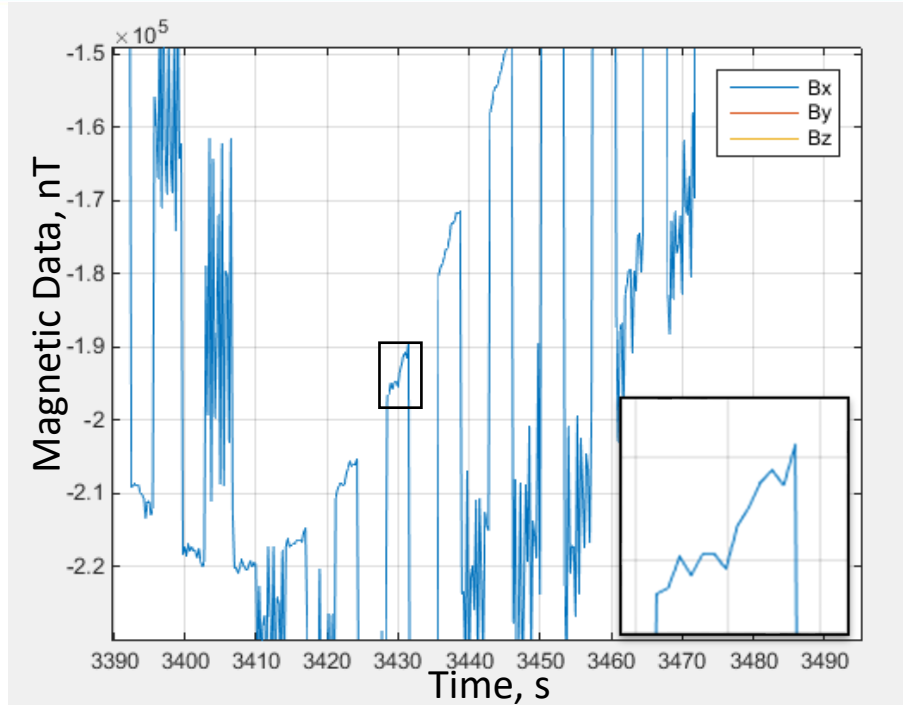
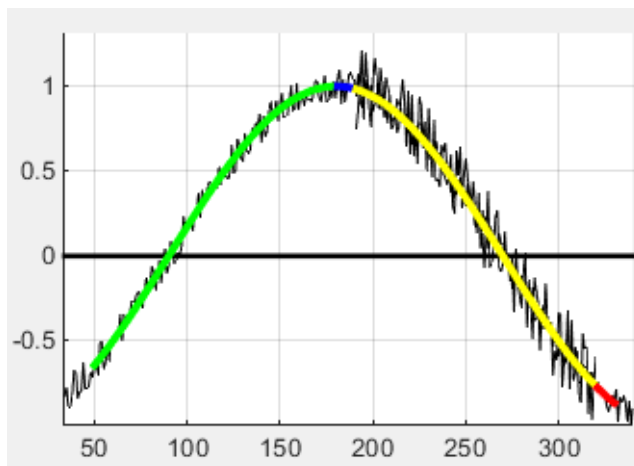
$$B(x) = a_0 + a_1x + a_2x^2$$

Derivative at the point

$$\dot{B}(x) = a_1 + 2a_2x$$

Required control current

$$J = -k^* \cdot (a_1 + 2a_2x_n)$$



Magnetometer measurements during algorithm work

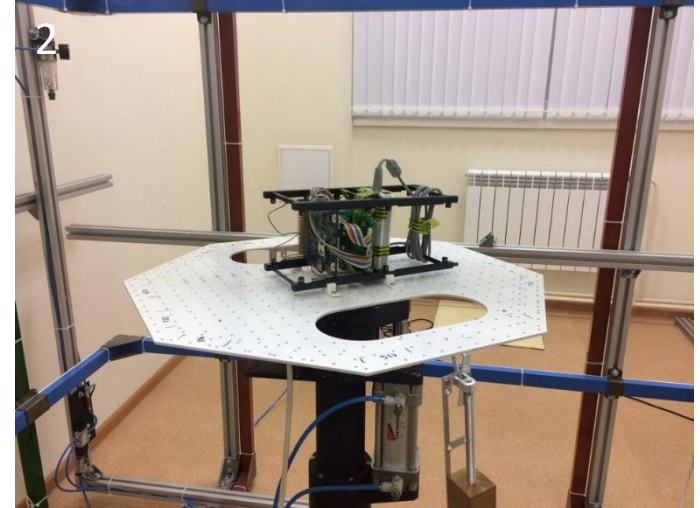
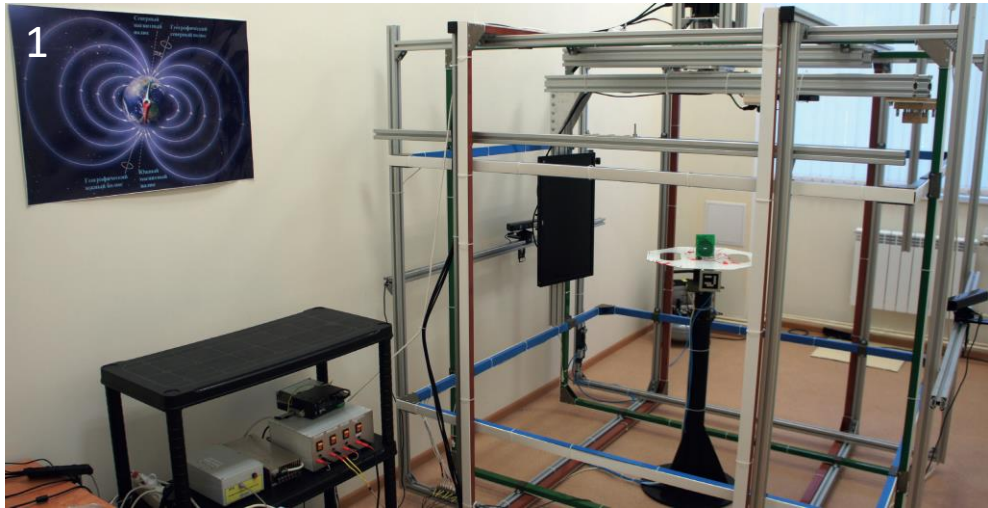


Algorithm work cycle

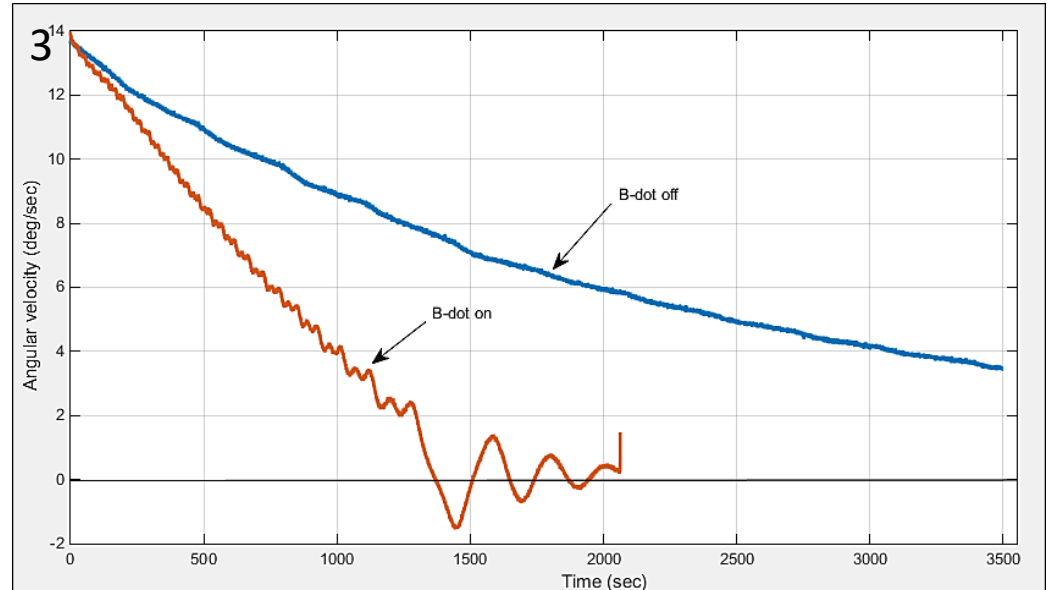
Magnetometer measuring step = 0.25 s



Damping Control. Testing

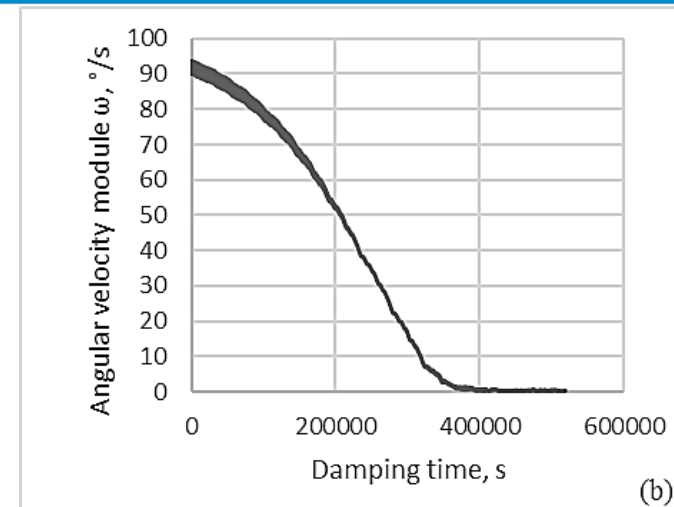
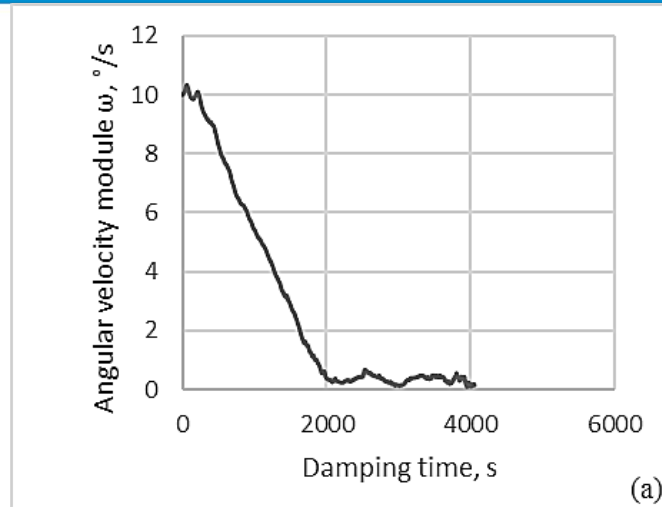


1. The Laboratory of the Nanosatellite Motion Control System Testing
2. The engineering model of the satellite, mounted on the rotating platform of the stand ($B=250$ nT)
3. Plots of the angular velocities of the engineering model for the cases: (blue) there is no damping; (red) damping is performed





Damping Control. Numerical Simulation



Damping time of initial angular velocities for nanosatellite SamSat-QB50

(a) initial angular velocity damping 10 deg/s; (b) initial angular velocity damping 90 deg/s

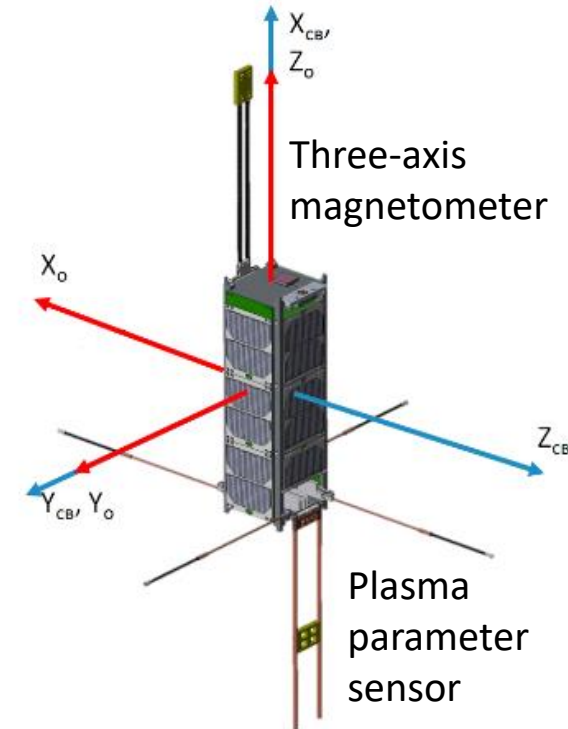
Algorithm work cycle at various angular speeds

Angular speed ω , deg / s	Koef., A m s/T	Time of measure, s	Time of control, s	Time of delay, s	Damping time, s
90	20000	1.5	1	0.25	23000 - 47000
80	20000	1.5	1	0.25	24000 - 33000
70	20000	1.5	1	0.25	15000 - 25000
60	20000	2	1.5	0.25	13000 - 18000
50	20000	2	2	0.25	10000 - 15000
40	20000	2	3	0.25	10000 - 13500
30	20000	3	4	0.25	5000 - 10000
20	20000	3	4	0.25	4000 - 5000
10	20000	3	4	0.25	2000 - 3000



SamSat-ION is being developed at the Samara University to study the Earth's upper ionosphere by contact and remote sensing methods in a sun-synchronous orbit with an inclination of 97.5 deg and an altitude of 550 km.

The main payload on the satellite is a plasma parameter sensor, the plane of which, for correct measurements, must be perpendicular to the incident flow vector. Thus, the nanosatellite needs **triaxial gravitational stabilization**.



Gravitational stabilized
SamSat-ION



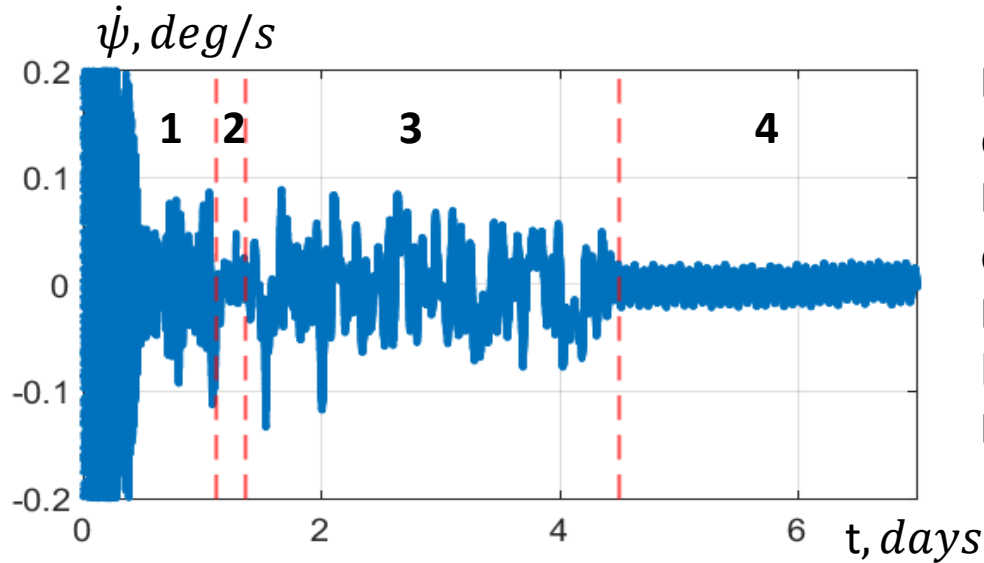
Mode 1 consists in damping the angular velocities of the nanosatellite using the B-dot algorithm, when the orbital velocity is reached, the algorithm switches to the next mode.

Mode 2 consists in keeping the angular velocity of the nanosatellite close to the orbital velocity using an algorithm ($\boldsymbol{\omega} \times \mathbf{B}$) for 6 hours.

Mode 3 consists in damping the angular velocities using **one coil**, which allows directing the control action into **one motion channel** and more precisely bringing the nanosatellite to a stable equilibrium position.



РЕЗУЛЬТАТЫ МОДЕЛИРОВАНИЯ С ИСПОЛЬЗОВАНИЕМ ДАННЫХ ОБ УГЛОВЫХ СКОРОСТЯХ

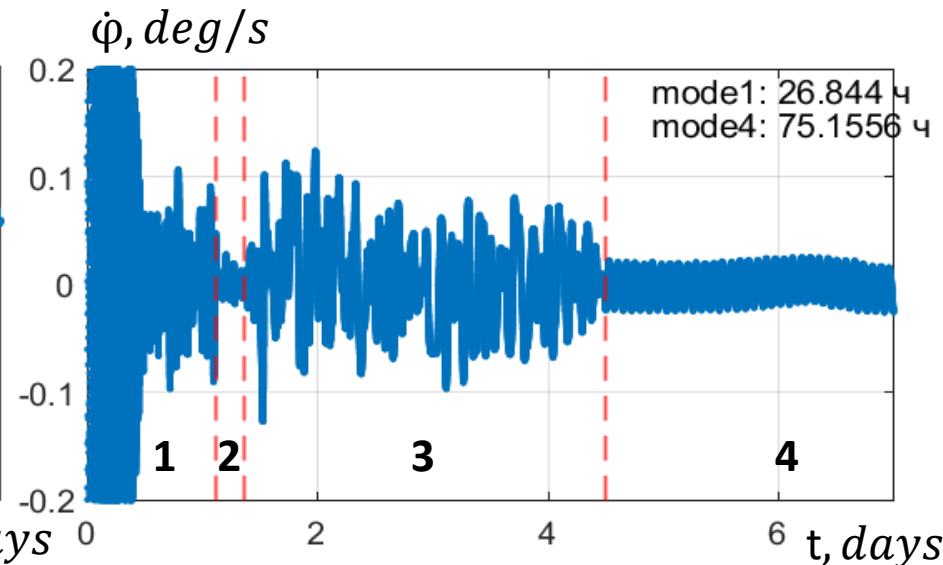
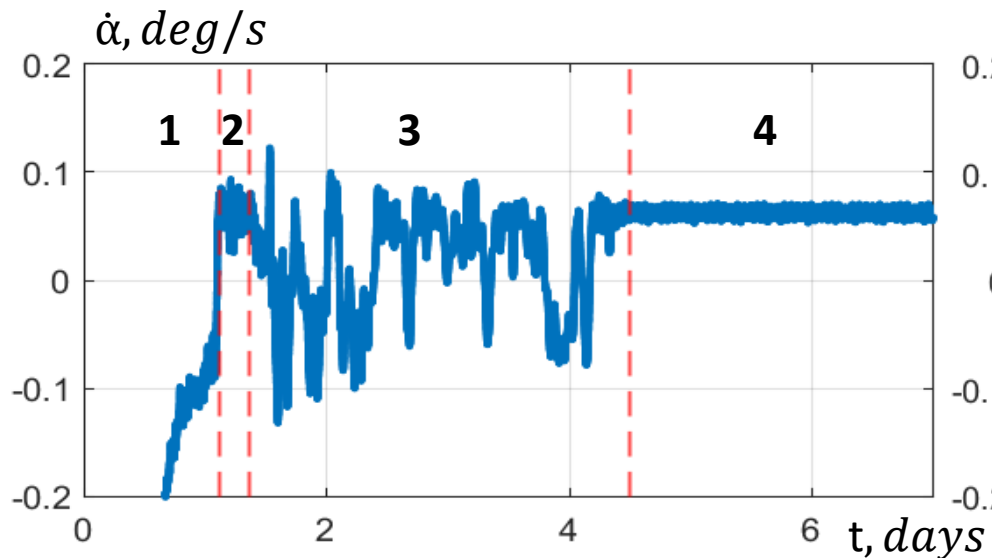


Mode 1: Damping of angular velocities $B \cdot \dot{\omega}$;

Mode 2: Keeping the angular velocity close to the orbital value ($\omega \times B$);

Mode 3: Damping using a single coil located on the Z-axis;

Mode 4: No control.





Three-axis stabilization

PD - Proportional-Differential

The output is a combination of how far you are from the goal and how fast you are moving towards the goal. The differential part is normally negative, this means that if you are rapidly approaching the goal then you start to slow down. It handles large changes well with minimal overshoot but isn't great for tracking small changes or errors. Good for systems which inherently have a lot of momentum.

Control momentum:

$$\mathbf{M}_{yp} = -k_{\omega}\boldsymbol{\omega} - k_a\mathbf{S}.$$

where k_{α} and k_{ω} - gains in the proportional and differential parts of the PD controller; $\bar{\omega}$ - angular velocity vector; $\bar{S} = (a_{23} - a_{32}, a_{31} - a_{13}, a_{12} - a_{21})^T$ - vector of orientation.



Ex 1. Momentum Wheel Control

1 Phase: Bias momentum state

The momentum wheel is used for controlling the attitude and angular rate of the satellite's pitch plane. Letting pitch angular rate and pitch angle of the body be ω_y and θ , the demanded control momentum is calculated as

$$M = k_p \theta + k_d \omega_y$$

where k_p ; k_d are control coefficients.

Possible to derive

$$\Delta\Omega = \frac{M \cdot \Delta T}{J} = \frac{(k_p \theta + k_d \omega_y) \cdot \Delta T}{J}$$

where ΔT is the sampling period. The control instruction of the momentum wheel is

$$\Omega = \Omega_{prev} + \Delta\Omega$$

where Ω_{prev} is the previous control instruction of rotational speed.

2 Phase: Zero-momentum controls yields

(three-axes magnetorquer unloads three-axes wheel)

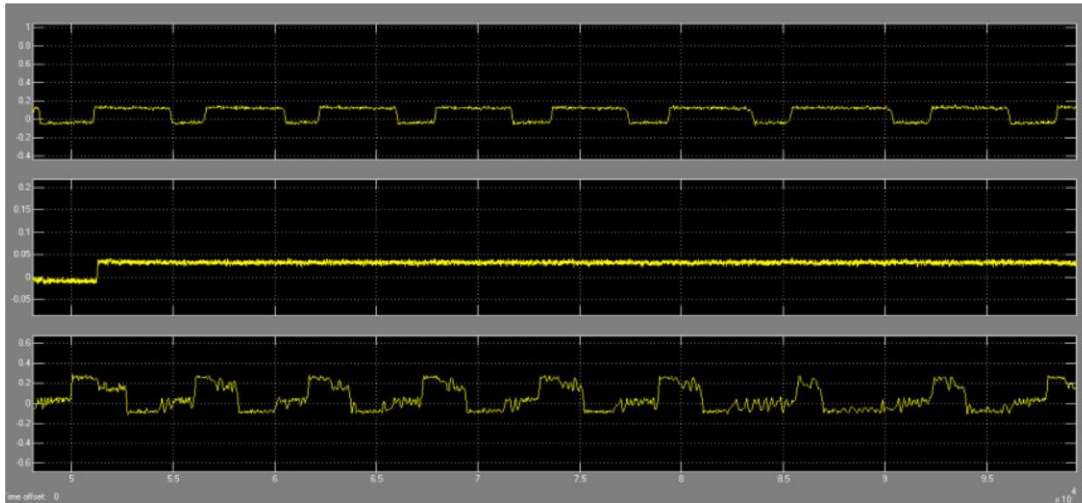
$$\mathbf{e} = \begin{bmatrix} e_x \\ e_y \\ e_z \end{bmatrix} = \begin{bmatrix} h_x \\ h_y \\ h_z \end{bmatrix} = \begin{bmatrix} J_{hx} \omega_{hx} \\ J_{hy} \omega_{hy} \\ J_{hz} \omega_{hz} \end{bmatrix}$$

$$\mathbf{M} = \mathbf{b}_b \times \mathbf{e}$$

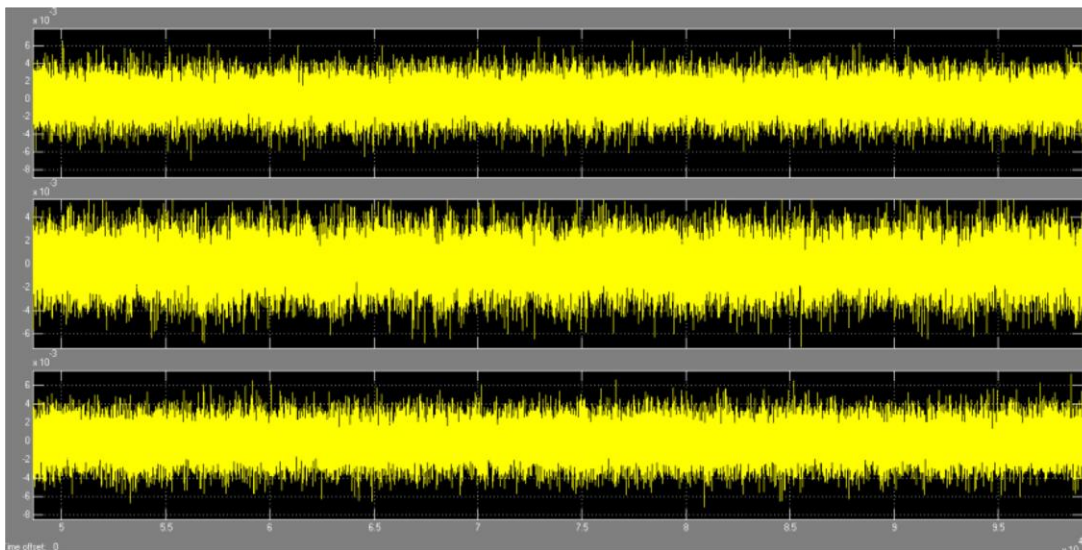
*<https://www.sciencedirect.com/science/article/pii/B9780128126721000035>



Three-axes attitude angle curve in control mode (degree)



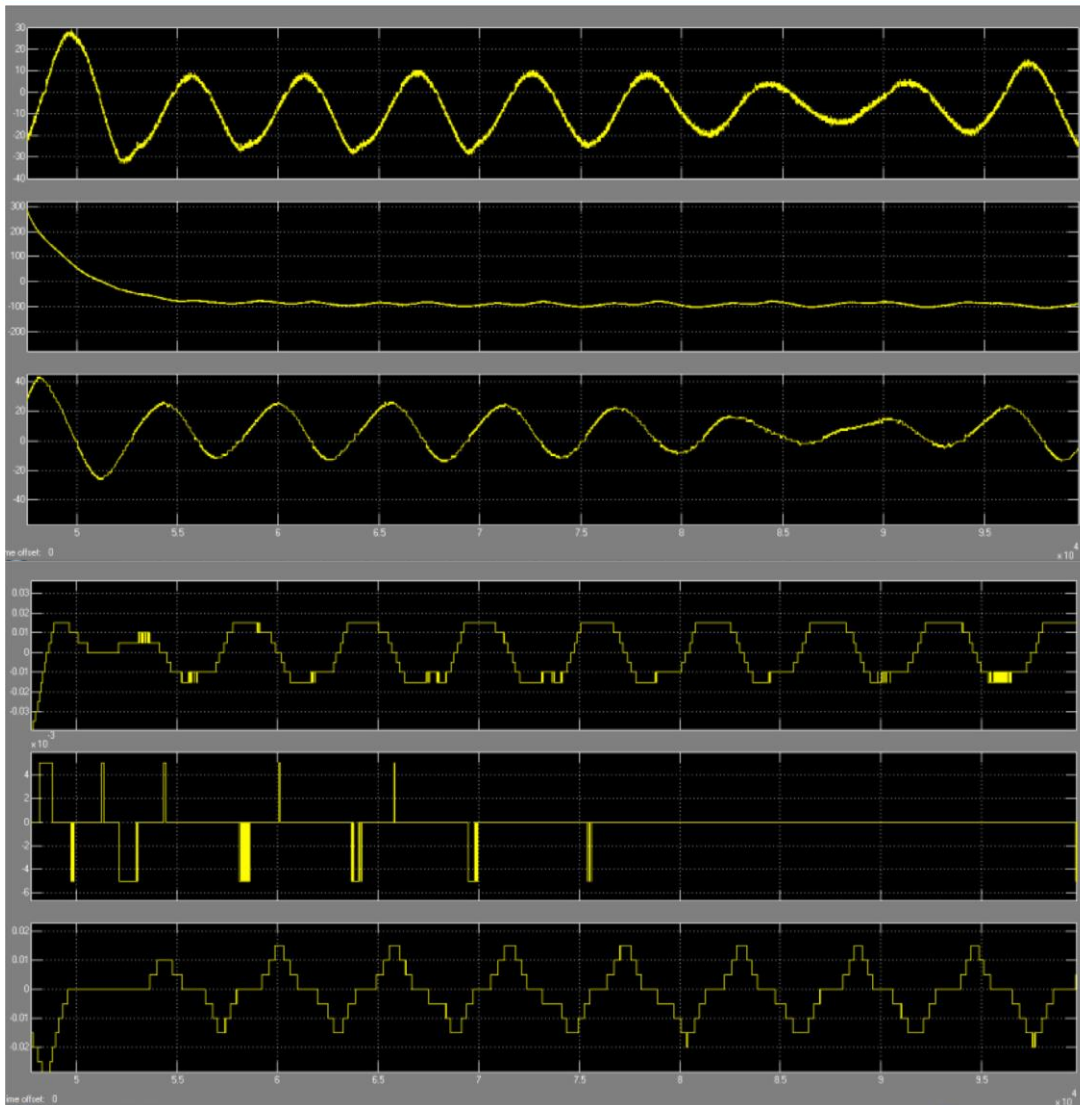
Estimation error curve of the three-axes attitude in control mode (degree)



*<https://www.sciencedirect.com/science/article/pii/B9780128126721000035>



Speed curve of the X, Y, Z wheel in control mode (rpm)



Magnetic torque output curve in control mode (Am^2)

*<https://www.sciencedirect.com/science/article/pii/B9780128126721000035>



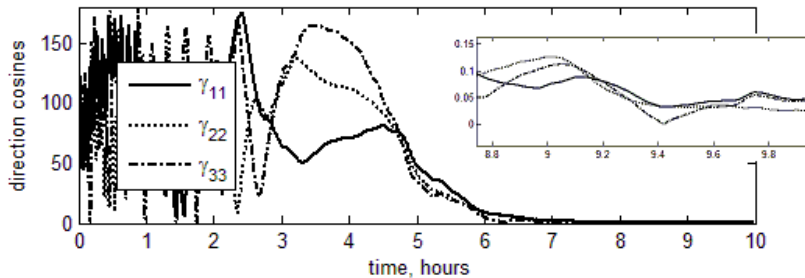
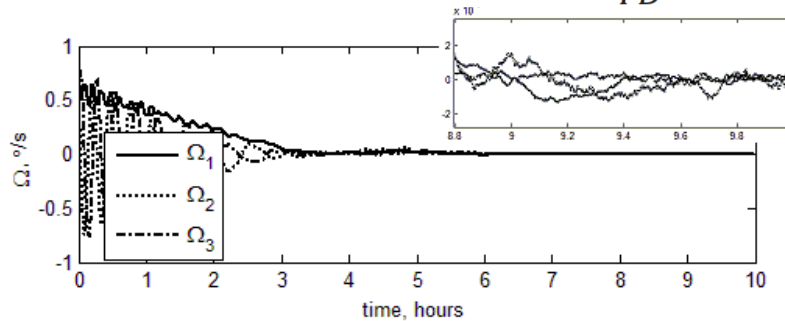
Ex 2. Magnetic Attitude Control

Projection of \mathbf{M} on the plane perpendicular to the local geomagnetic induction vector is used for implementing this torque with magnetorquers,

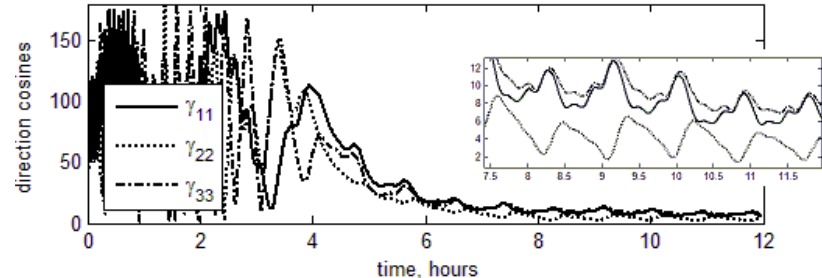
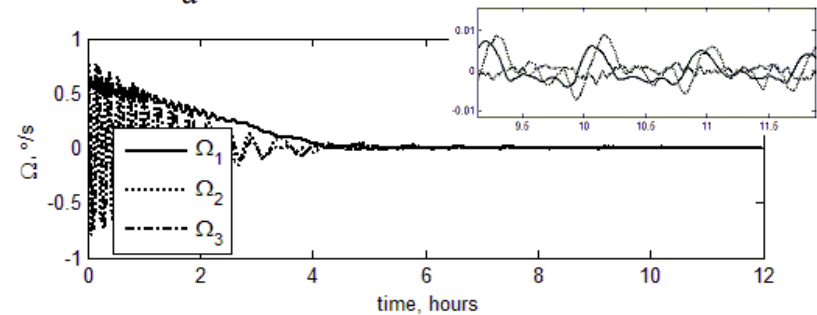
$$\mathbf{M} = (\mathbf{B} \times \mathbf{M}_{PD}) \times \mathbf{B}.$$

Dipole magnetic moment constructed as

$$\mathbf{m} = \mathbf{B} \times \mathbf{M}_{PD} = -k_{\omega} \mathbf{B} \times \boldsymbol{\omega} - k_a \mathbf{B} \times \mathbf{S}.$$



Three-axis stabilization simulation,
Gaussian disturbance



Three-axis stabilization simulation,
constant and Gaussian disturbance,
inertia tensor error

*<http://library.keldysh.ru/preprint.asp?id=2015-47&lg=e>

**<https://www.sciencedirect.com/science/article/pii/S0094576514004640>

Moskovskoye shosse, 34, Samara, 443086, Russia, tel.: +7 (846) 335-18-26, fax: +7 (846) 335-18-36, www.ssau.ru, e-mail: ssau@ssau.ru



САМАРСКИЙ УНИВЕРСИТЕТ
SAMARA UNIVERSITY

THANK YOU

Petr Nikolaev
pnikolayev@gmail.com

34, Moskovskoye shosse, Samara, 443086, Russia
Tel.: +7 (846) 335-18-26, факс: +7 (846) 335-18-36
www.ssau.ru, e-mail: ssau@ssau.ru